J. Fluid Mech. (1965), *vol.* 22, *part* 1, *pp.* 161–186
Printed in Great Britain

Turbulent jets in ducted streams

By PHILIP G. HILL
Department of Mechanical Engineering, Massachusetts Institute of Technology

(Received 2 April 1964 and in revised form 11 September 1964)

An attempt has been made to predict the mean velocity field of turbulent jets immersed in secondary streams confined by constant-area ducts. The calculations have employed empirical data derived solely from the turbulent free jet. The conditions under which ducted jets may be considered approximately self-preserving have been examined by comparison of results of momentum-integral calculations with data from various sources on two-dimensional and axisymmetric jets immersed in secondary streams of constant velocity. For flows in which confining walls have significant effects, it is shown that the velocity field may be determined fairly well from free-jet data using the assumption of approximate self-preservation. Before the jet spreads to the wall, both the mean-velocity and turbulent shear stress are assumed self-preserving. Afterward only the shear stress is subject to this condition. Improvement of the methods used appears mainly to require a better model of the zone of recirculation.

1. Introduction

The experimental behaviour of the free turbulent jet, i.e. one which issues into a large stationary body of the same fluid, is now quite well known (see, for example, Townsend 1956, Hinze 1959, Schlichting 1958). Numerous measurements have been made of mean and fluctuating velocities, temperatures and concentrations of chemical species. Much less well known is the behaviour of the jet immersed in a secondary stream, especially when the effects of confining walls are important. These effects are particularly significant in ejectors and certain combustors in which the flame is stabilized by a recirculating flow of combustion products.

The two-dimensional, or plane, jet immersed in a secondary stream of approximately uniform and constant velocity has been studied experimentally by Weinstein, Osterle & Forstall (1956). His results, for various ratios of secondary and jet velocities, have been shown by Spalding (1958) to be essentially functions of a single independent variable. Ferguson (1949) has measured the mean velocity field of a two-dimensional jet immersed in a duct. Curtet (1958) has also reported measurements for this case, and Craya & Curtet (1955) have developed a method of calculating the flow field assuming the external stream to be a potential flow.

Experimental data on the axisymmetric jet in an external stream of approximately constant velocity have been provided by Forstall & Shapiro (1950), Landis & Shapiro (1951) and Pabst (1944). Using Prandtl's mixing length theory, Squire & Trouncer (1944) and Szablewski (1946) have developed momentum

integral equations with which to calculate the flow field. Considerable data has been provided by Hembold, Luessen & Heinrich (1954) and Becker, Hottel & Williams (1962) for confined axisymmetric flows on which the walls exert a dominating influence.

Little experimental information on turbulent shear stresses is available for jet flows other than the free jet. Extensive measurements on the free jet have shown that this flow is closely self-preserving. The measurements of Corrsin on the axisymmetric free jet, for example, have shown that the mean velocity distribution becomes nearly self-preserving within eight diameters from the nozzle. From this, and the observation that the jet spreading is very nearly linear with

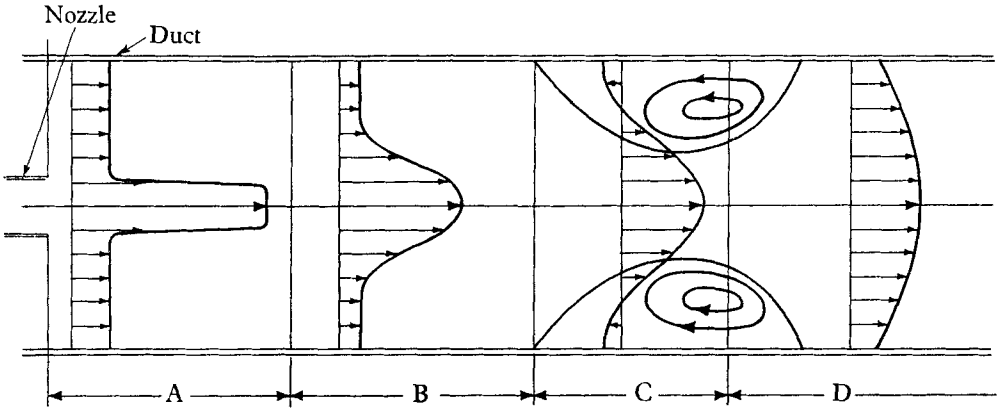

FIGURE 1. Flow régimes.

axial distance, it may be deduced that the turbulent shear stress distribution is also closely self-preserving. Thus, in contrast with other jet flows, the free-jet velocity and shear stress distributions are well known. The purpose of this paper is to show that, under certain conditions, the mean velocity field of the ducted turbulent jet may be predicted quite well from free-jet data, using no other empirical information.

Figure 1 illustrates the behaviour of a jet in an axisymmetric duct of uniform cross-sectional area. Ignoring the effects of the wall boundary layers, at least four idealized regions of flow may be identified.

(A) A transition region in which the jet velocity distribution develops a nearly constant shape. In the flows of interest herein this region is short (of the order of eight to twenty nozzle diameters).

(B) A region in which the external stream may be considered a potential flow and the jet velocity and shear stress distributions may be considered approximately self-preserving. As the jet spreads it entrains fluid from the external stream rapidly enough to reduce the free-stream velocity and thus a positive axial pressure gradient is established.

(C) A possible region of recirculation. If the jet entrains all the free-stream fluid before spreading to the wall, a zone of recirculating flow will be established. Experimentally it has been found that even in this region the jet velocity profile is still of approximately constant shape. The flow outside the jet can no longer be

considered potential because it consists of fluid recirculating through the jet itself. This zone may, to a first approximation, be considered uniform in pressure up to the point at which the jet shear layer approaches the wall.

(D) A region downstream of the point at which the jet attaches to the wall. Considerable pressure gradients may be established in this zone and the flow can no longer be considered even approximately self-preserving (although the eddy viscosity distribution retains approximate similarity).

Self preservation

The main terms of the Reynolds equations for free turbulent shear flow are, at sufficiently high Reynolds numbers,

$$U\frac{\partial U}{\partial x}+V\frac{\partial U}{\partial y}+\frac{1}{y^i}\frac{\partial(\overline{uv}y^i)}{\partial y}+\frac{1}{\rho}\frac{dP}{dx}=0 \quad (i=0,1), \tag{1}$$

in which $P=p+\rho\overline{u^2}$ and the symbols are defined as follows:

The index i is zero for two-dimensional flow and one for axisymmetric flow. The x- and y-directions are parallel and normal, respectively, to the jet axis. The mean velocities in the x- and y-directions are U and V and the corresponding fluctuating velocities are u and v. The static pressure is denoted by P. The Reynolds shear stress is

$$\tau=-\rho\overline{uv}.$$

When the stream outside the jet may be considered a potential flow the pressure gradient dP/dx is given by

$$\frac{1}{\rho}\frac{dP}{dx}=-U_0\frac{dU_0}{dx},$$

assuming $(\overline{u^2}-\overline{v^2})\ll U_0$.

If the jet flow is assumed to be self-preserving then the velocity and shear distributions may be expressed as

$$(U-U_0)/U_j=f(y/\delta), \tag{2}$$

$$\tau/\rho U_j^2=g(y/\delta). \tag{3}$$

As illustrated in figure 2, U_0 is the free-stream velocity, U_j the difference between jet maximum velocity and free-stream velocity, and δ is the distance from the centre-line of the jet to its edge. Another jet thickness b, the width of the jet between points at which the velocity is midway between U_0 and (U_0+U_j), will be used later.

The continuity condition is

$$\partial(Uy^i)/\partial x+\partial(Vy^i)/\partial y=0 \quad (i=0,1).$$

Defining $\lambda=U_0/U_j$ and $\eta=y/\delta$, and substituting these similarity expressions and the continuity relation in equation (1) the result may be expressed in the form

$$\frac{1}{U_j}\frac{dU_j}{dx}\left[\lambda f+f^2-\frac{f'}{\eta^i}\int_0^\eta f\eta_1^i\,d\eta_1\right]+\frac{1}{U_0}\frac{dU_0}{dx}\left[\lambda f-\frac{\lambda f'\eta}{1+i}\right]$$
$$+\frac{1}{\delta}\frac{d\delta}{dx}\left[-\lambda f'\eta-(1+i)\frac{f'}{\eta^i}\int_0^\eta f\eta_1^i\,d\eta_1\right]=\frac{1}{\delta\eta^i}\frac{\partial}{\partial n}(g\eta^i). \tag{4}$$

Since λ, U_j and δ are functions of x the only conditions under which f and g can be considered universal functions of η are

$$\lambda \ll 1 \quad \text{or} \quad \lambda \gg 1.$$

For the case $\lambda \ll 1$ it may be shown that even if U_0 is variable, self-preservation of the flow implies

$$\left.\begin{aligned} \delta &\propto x \quad (i = 0, 1), \\ U_j &\propto x^{-\frac{1}{2}} \quad (i = 0), \\ &x^{-1} \quad (i = 1), \end{aligned}\right\} \tag{5}$$

where x is the distance from the virtual origin.

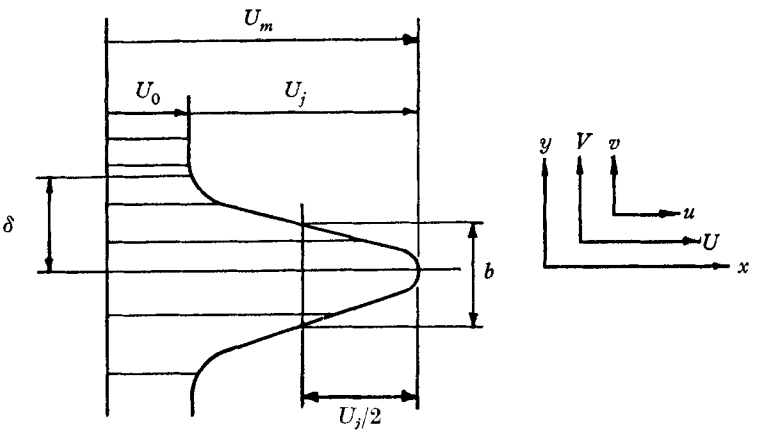

FIGURE 2. Nomenclature for velocity distribution.

For the other case, $\lambda \gg 1$, it may be shown (e.g. Townsend 1956) that if U_0 is constant,

$$\begin{aligned} \delta &\propto x^{\frac{1}{2}} \quad (i = 0), \\ &\propto x^{\frac{1}{3}} \quad (i = 1), \\ U_j &\propto x^{-\frac{1}{2}} \quad (i = 0), \\ \text{and} \qquad &\propto x^{-\frac{2}{3}} \quad (i = 1). \end{aligned}$$

2. Free jet ($\lambda = 0$)

Figure 3 shows data on the velocity distribution of the axisymmetric free turbulent jet and a mean curve used in calculations to be described herein. Figure 4 shows data on the rate of spreading of the free jet; it becomes linear quite close to the nozzle. Thus, for the case $\lambda = 0$, equation (5) is satisfied to the accuracy of experimental data and it may be concluded that equations (2) and (3) are legitimate assumptions.

The conditions under which equations (2) and (3) (with $f(\eta)$ and $g(\eta)$ evaluated from free-jet data) are satisfactory for $\lambda \neq 0$ can be examined by comparing the results of calculations, based on these assumptions, on immersed jets with (i) data on jets in constant velocity streams, (ii) data on jets in ducted streams.

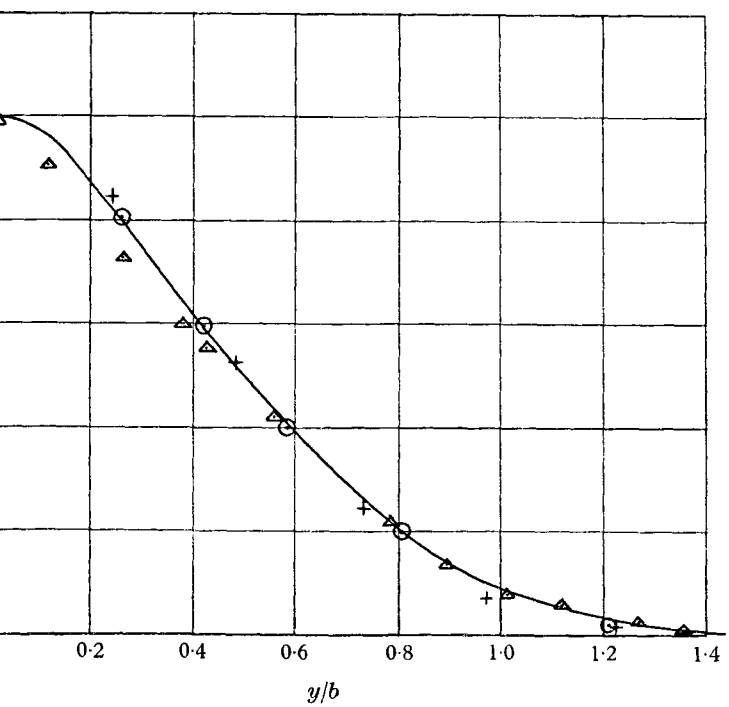

E 3. Free-jet velocity distribution. (Adapted from Townsend 1956.)
⊙, Corrsin & Uberoi; +, Corrsin; △, Reichardt; —, mean.

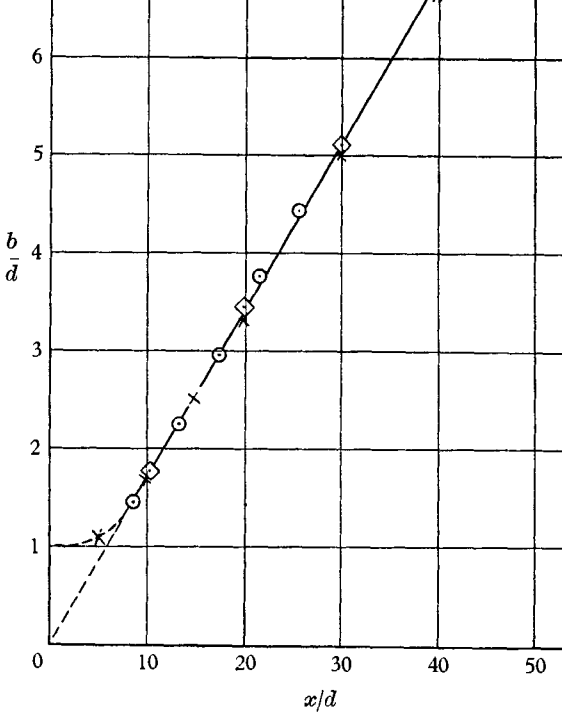

FIGURE 4. Free-jet spreading (after Townsend 1956). ⊙
& Uberoi; ×, Corrsin; ◇, Hinze & Van der Hegge Z

3. Jets in constant velocity streams

Momentum integral equations

The momentum thickness θ is defined by

$$U_0^2\theta^{(1+i)} = 2\pi^i \int_0^\infty U(U-U_0)y^i\,dy.$$

If the velocity distribution conforms to equation (2) then

$$\frac{\theta}{\delta} = \left[2\pi^i\left\{\lambda\int_0^1 f\eta^i\,d\eta + \int_0^1 f^2\eta^i\,d\eta\right\}\Big/\lambda^2\right]^{1/(1+i)} \tag{6}$$

If the pressure is uniform, θ will be constant for the whole flow, regardless of whether self-preservation applies. For a rectangular velocity profile in the exit plane of the nozzle, equation (6) may be written

$$\frac{\theta}{d} = \left[\left(\frac{\pi}{4}\right)^i\left(\frac{\lambda_0+1}{\lambda_0^2}\right)\right]^{1/(1+i)},$$

in which d is the diameter of the nozzle and λ_0 is the velocity ratio at its exit plane.

If the flow is held to be approximately self-preserving and $f(\eta)$ is known, equation (6) relates local values of λ and δ. Another relationship is needed to determine the axial variation of these two quantities. It may be obtained in several ways.

The momentum equation could be integrated across a zone whose width is only half the distance between the edge and the centre-line of the jet. This would require evaluation of the turbulent shear stress on one surface of the arbitrary control volume. Such a method has been adopted by Squire & Trouncer (1944) who used the mixing-length theory to relate this shear stress to the local velocity gradient.

Another method, used by Truckenbrodt (see Schlichting 1958) for boundary layers, consists of multiplying the momentum equation by U and integrating across the whole zone to form an energy integral equation which contains an integral of the shear stress.

The method used herein consists of multiplying the momentum equation by y^{1+i} and then integrating across the whole zone to form a moment-of-momentum integral equation which contains the integral of the shear stress distribution mentioned previously. It may be noted that Tetervin & Lin (1951) have obtained relations for the general case in which the momentum equation is multiplied by $U^m y^n$ (m and n being integers) and integrated across the whole layer.

Curtet (1958) has used a more complex procedure for obtaining integral equations. First he integrates the momentum equation between the centre-line and a general value of η. Then he approximates the result and multiplies it by a certain function of η before integrating across the whole layer.

The choice between the methods used by Squire & Trouncer, and Truckenbrodt, and the present one is arbitrary in the sense that if the exact solution were known it must satisfy all three equations. Fortunately, experience indicates that the

choice between them is not very important. For example, it may be shown that if identical velocity profiles and the mixing-length theory are assumed in order to calculate the rate of spreading of the turbulent wake, the difference between the Squire & Trouncer and present methods in the prediction of spreading rate is only a few per cent.

The present method has the advantage over that of Squire & Trouncer of not requiring the choice of an arbitrary limit for the second integral of the momentum equation. Also, it does not require the use of a phenomenological theory to relate the shear stress at that boundary to the local velocity gradient.

It may at first appear that multiplying the momentum equation by y^{1+i} and then integrating across the whole zone provides an effective weighting factor for conditions in the outer part of the jet. However, it may be shown from subsequent equations that an identical result is obtained by multiplying by $(\delta-y)y^i$ before integrating. The choice of axis around which the moments of momentum and pressure forces are summed has no effect on the solution, as is well known for problems involving only static forces.

Proceeding then to form a moment-of-momentum integral equation by multiplying equation (4) by η^{1+i} and integrating across the entire jet, the result is (for constant U_0)

$$\frac{1}{U_j}\frac{dU_j}{dx}[\lambda\phi_{1i}+\phi_{2i}+\phi_{3i}]+\frac{1}{\delta}\frac{d\delta}{dx}[(2+i)\lambda\phi_{1i}+(1+i)\phi_{3i}]=\frac{\psi_i}{\delta} \quad (i=0,1), \tag{7}$$

in which
$$\phi_{1i}=\int_0^1 f\eta^{1+i}\,d\eta, \qquad \phi_{2i}=\int_0^1 f^2\eta^{1+i}\,d\eta,$$

$$\phi_{3i}=-\int_0^1 \eta f'\int_0^\eta f\eta_1^i\,d\eta_1\,d\eta \qquad \text{and} \qquad \psi_i=\int_0^1 \eta\frac{\partial}{\partial\eta}\left(\frac{\tau\eta^i}{\rho U_j^2}\right)d\eta.$$

Defining also
$$\phi_{4i}=\int_0^1 f\eta^i\,d\eta \quad \text{and} \quad \phi_{5i}=\int_0^1 f^2\eta^i\,d\eta$$

permits equation (6) to be written

$$\frac{\theta}{\delta}=\left[2\pi^i\frac{(\lambda\phi_{4i}+\phi_{5i})}{\lambda^2}\right]^{1/(1+i)} \tag{8}$$

Equations (7) and (8) show that, as long as the flow is self-preserving and U_0 is constant, the velocity ratio $\lambda = U_0/U_j$ and the thickness ratio δ/θ both depend only on x/θ. Spalding has deduced this dependence by a more general argument. Hypothesizing that the jet has essentially 'forgotten' the upstream conditions, its local rate of change depends only on local conditions. He postulated that, for example,

$$dU_j/dx = h(\dot{M}, \rho, U_j, U_0),$$

in which $\dot{M}$ is the excess momentum of the jet. For the axisymmetric case

$$\dot{M}=\int_0^\infty 2\pi\rho U(U-U_0)\,dy.$$

Using dimensional analysis, and recognizing that U_0 and $\dot{M}$ are constants, allows this relationship to be written in the form

$$\frac{d\lambda}{d(x/\theta)} = M(\lambda),$$

in which

$$\theta = \left(\frac{\dot{M}}{U_0^2\rho}\right)^{\frac{1}{2}}.$$

Thus $\lambda = \lambda(x/\theta)$.

Equations (7) and (8) will now be combined for both axisymmetric and two-dimensional (plane) jets. Based on free-jet data and the self-preservation assumption, the flow will be calculated for general values of λ. The results will then be compared with experimental data to see under what conditions the method appears to be reliable.

Axisymmetric jet in a constant velocity stream

Using equations (8) to eliminate δ from equation (7) for $i = 1$ yields an expression which, when integrated, becomes

$$\frac{x}{\theta} = \frac{\phi_{11}}{\psi_1(2\pi)^{\frac{1}{2}}\phi_{41}^{\frac{1}{2}}}\left[\frac{\Lambda^{\frac{3}{2}}}{3} + 2\left(\frac{\phi_{51}}{\phi_{41}} - \frac{\phi_{21}}{\phi_{11}}\right)\Lambda^{\frac{1}{2}} + 2\frac{\phi_{51}}{\phi_{41}}\left(\frac{3}{2}\frac{\phi_{51}}{\phi_{41}} - \frac{\phi_{31}}{\phi_{11}}\right)\Lambda^{-\frac{1}{2}}\right] + C_1, \qquad (9)$$

in which $\Lambda = \lambda + \phi_{51}/\phi_{41}$ and C_1 is a constant of integration. The integrals $\phi_{11}, \ldots, \phi_{51}$, which depend only on the velocity distribution, have already been defined as well as the shear integral ψ_1. The momentum thickness θ may be obtained from conditions at the nozzle exit,

$$\theta/d = \{\tfrac{1}{4}\pi(\lambda_0 + 1)/\lambda_0^2\}^{\frac{1}{2}},$$

in which d is the nozzle diameter and λ_0 the initial velocity ratio.

Instead of assuming the velocity distribution $f(\eta)$ to be a Gaussian or other simple function derived from the application of the phenomenological theories to jets, the integrals $\phi_{11}, \ldots, \phi_{51}$ may be evaluated directly from free-jet velocity measurements. From the mean curve of figure 3 the following values were obtained.

$$\phi_{11} = 0{\cdot}0378, \quad \phi_{21} = 0{\cdot}0124, \quad \phi_{31} = 0{\cdot}0228,$$
$$\phi_{41} = 0{\cdot}0950, \quad \phi_{51} = 0{\cdot}0445.$$

The shear stress integral ψ_1 may be determined from free-jet data as follows. For $\lambda = 0$ and $i = 1$ the conservation of momentum requires $U_j^2\delta^2 = \text{const.}$, or

$$\frac{1}{U_j}\frac{dU_j}{dx} = -\frac{1}{\delta}\frac{d\delta}{dx},$$

and equation (7) with the use of this relation becomes

$$\psi_1 = (\phi_{31} - \phi_{21})\,(d\delta/dx)_{\lambda=0}.$$

Figure 4 shows data for the spreading of the free jet. The location of the virtual origin is close indeed to the exit plane of the nozzle. The jet width b used in figure 4 is the diameter between points at which the fluid velocity is half the

maximum velocity. Using the mean velocity curve of figure 3, $\delta \approx 1{\cdot}44b$. Then using figure 4 to obtain $db/dx \approx 0{\cdot}170$ the above relationship yields

$$\psi_1 = 0{\cdot}00255.$$

As an independent check ψ_1 may be used to compute free-jet entrainment which Ricou & Spalding (1961) have measured accurately and reported in the form

$$m_1/x(M_1\rho)^{\frac{1}{2}} = 0{\cdot}282,$$

in which m_1 is the mass flux of the jet and M_1 the momentum flux. If the jet is assumed self-preserving

$$\frac{m_1}{x(M_1\rho)^{\frac{1}{2}}} = \frac{(2\pi)^{\frac{1}{2}}\delta}{x}\frac{\phi_{41}}{\phi_{51}^{\frac{1}{2}}}$$

or

$$\frac{m_1}{x(M_1\rho)^{\frac{1}{2}}} = \frac{(2\pi)^{\frac{1}{2}}\psi_1\phi_{41}}{(\phi_{31}-\phi_{21})\phi_{51}^{\frac{1}{2}}}.$$

Using the values of ϕ_1, ϕ_{21}, ϕ_{31}, ϕ_{41}, ϕ_{51} already given the result is

$$m_1/x(M_1\rho)^{\frac{1}{2}} = 0{\cdot}276,$$

which is close indeed to the Ricou & Spalding value.

Having evaluated $\phi_{11}, \ldots, \phi_{51}$ and ψ_1 the constant of integration C_1 in equation (9) may be determined by the condition that at the virtual origin $x = 0$ and $\lambda = 0$. After evaluating coefficients equation (9) becomes

$$x/\theta = 6{\cdot}39\Lambda^{\frac{3}{2}} + 5{\cdot}38\Lambda^{\frac{1}{2}} + 1{\cdot}76\Lambda^{-\frac{1}{2}} - 8{\cdot}30, \tag{10}$$

in which

$$\Lambda = \lambda + 0{\cdot}468.$$

Since λ is thus given as a function of x/θ the thickness ratio δ/θ or b/θ can similarly be related to x/θ by applying equation (8) for $i = 1$:

$$\delta/\theta = \lambda/\{2\pi(\lambda\phi_{41} + \phi_{51})\}^{\frac{1}{2}}.$$

Figures (5) and (6) show the predictions of λ and b/θ which can be made in this way.

Experimental data

Figures 5 and 6 also show the data reported by Landis & Shapiro (1951) and Pabst (1944) for axisymmetric jets in a moving external stream. Both the Landis–Shapiro and Pabst experiments were conducted with heated jet streams. To take into account the first-order effects of density difference between jet and secondary streams the momentum thickness is modified to read

$$\frac{\theta}{d} = \left\{\frac{\pi}{4}\frac{\rho_j}{\rho_0}\frac{\lambda_0+1}{\lambda_0^2}\right\}^{\frac{1}{2}},$$

in which ρ_j/ρ_0 is the ratio of jet density to secondary stream density. The Mach number of the Pabst jet was approximately 0·84.

The virtual origin of the Pabst jet was assumed to be in the exit plane of the jet since detailed measurements showed the velocity distributions to be quite close to rectangular at that plane. The virtual origin of the Landis & Shapiro jets

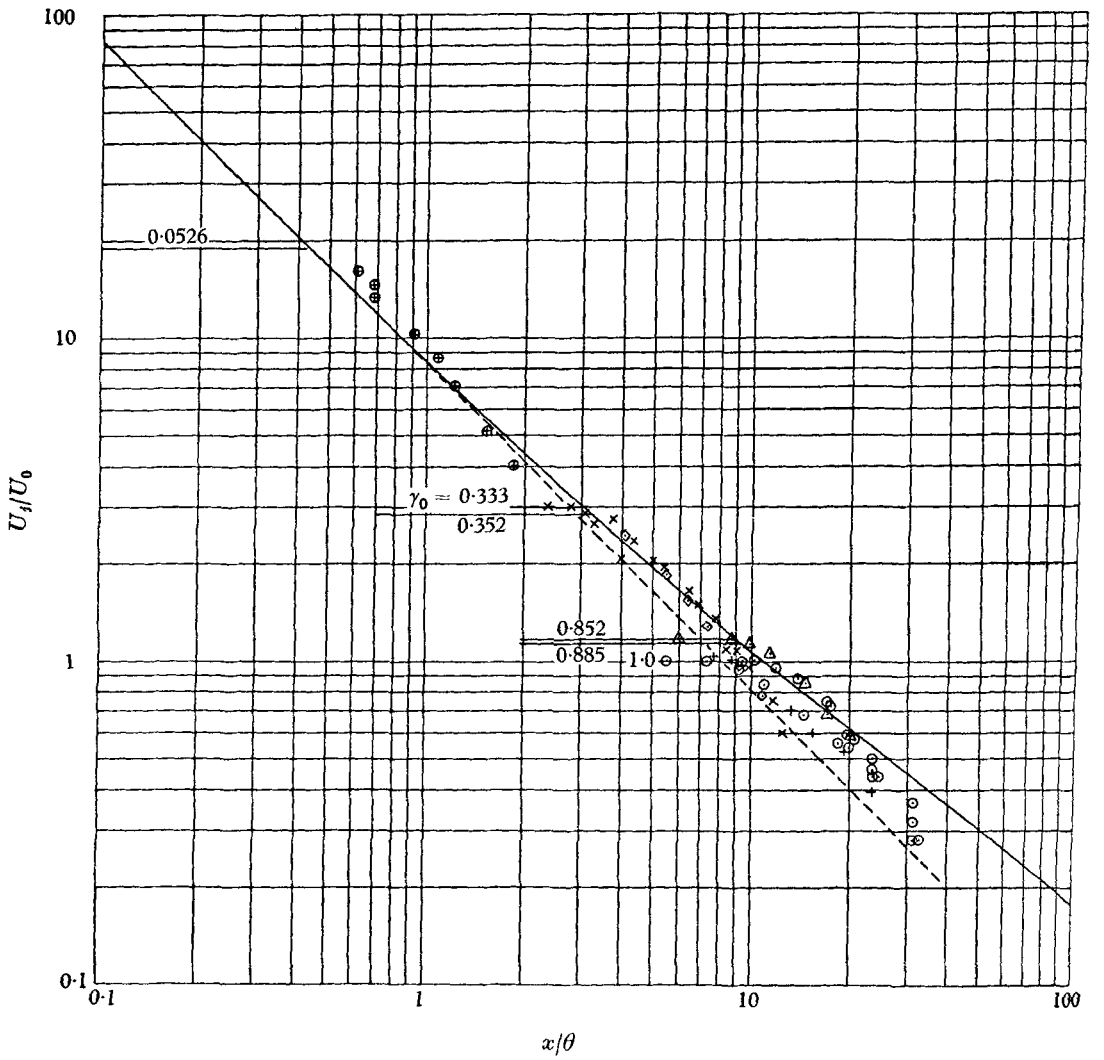

FIGURE 5. Axisymmetric jets in moving streams. λ_0 (Landis–Shapiro): ×, 0·333; △, 0·852; ⊙, 0; ⊕, 0·0562 (Pabst); ◇, 0·352; +, 0·885; —, theoretical; – – –, $U_j \propto x^{-1}$,

$$\frac{\theta}{d} = \sqrt{\left\{\frac{\pi}{4}\frac{\rho_j}{\rho_0}\left(\frac{\lambda_0+1}{\lambda_0^2}\right)\right\}}.$$

has been determined in the following way. Figure 4 indicates that the length of the potential core for the free jets measured by Corrsin, Corrsin & Uberoi and Hinze & Van der Hegge Zijnen (see Townsend 1956) is about eight diameters from the nozzle exit plane. On the other hand, Forstall & Shapiro (1950) report (from measurements made on the same apparatus, and consistent with those of Landis & Shapiro) that the core length is given by

$$x/d = 4 + 12\mu,$$

in which μ is the ratio of secondary to jet maximum velocity. This predicts that for the free-jet case ($\lambda = \mu = 0$) the core length is only four diameters. The discrepancy between this value and the one obtained from figure 4 could be due to the nozzle exit velocity profile being considerably more rounded in one case than the other, and suggests that the virtual origin should be shifted four diameters upstream of the nozzle exit plane as has been done for the Landis–Shapiro data shown in figures 5 and 6. In the absence of contrary information, the virtual origin of the jet will be assumed independent of the velocity ratio λ.

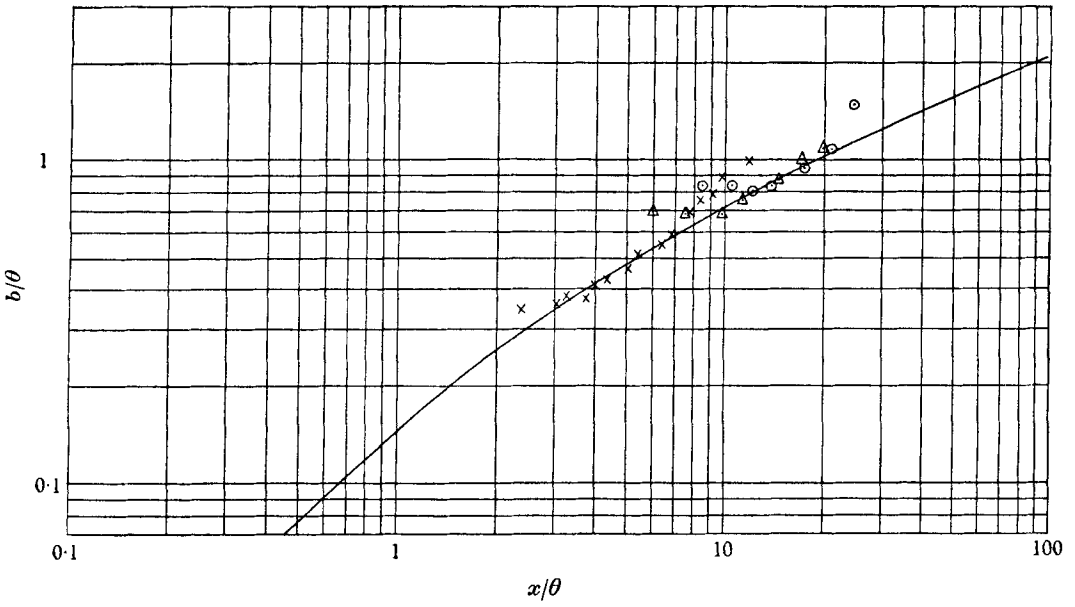

FIGURE 6. Axisymmetric jets in moving streams. λ_0 (Landis–Shapiro): ×, 0·333; △, 0·852; ⊙, 1·0; —, theoretical,

$$\frac{\theta}{d} = \sqrt{\left\{\frac{\pi}{4}\frac{\rho_j}{\rho_0}\left(\frac{\lambda_0+1}{\lambda_0^2}\right)\right\}}.$$

Figures 5 and 6 reveal that on the whole the assumption of approximate self-preservation leads to quite a good prediction of the general case from free-jet data. Figure 5 indicates that for values of λ exceeding unity the prediction begins to deviate from the measured data. This point will be discussed further after corresponding results for the two-dimensional or plane jet have been examined. Figures 5 and 6 also indicate increasing discrepancy between the results of calculation and equations (5) which are the consequences of self-preservation. Thus, above a value of unity the flow cannot be considered even approximately self-preserving.

Two-dimensional (plane) jet in a constant-velocity stream

In the same way as for the axisymmetric jet the behaviour of the two-dimensional (plane) jet may be calculated as shown in the Appendix. Figures 7 and 8 show the results of these calculations and the data of Weinstein for the two-dimensional

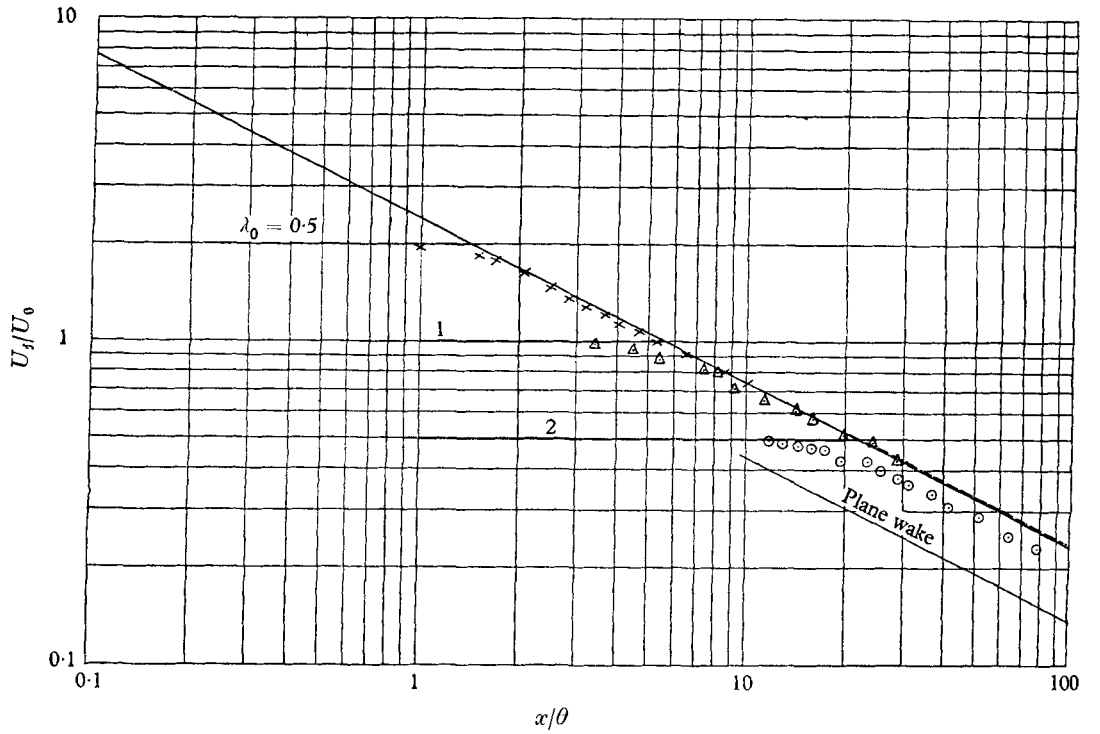

FIGURE 7. Plane jets in moving streams.
λ_0 (Weinstein): ×, 0·5; △, 1; ⊙, 2; —, theoretical, $\theta/d = (\lambda_0+1)/\lambda_0^2$.

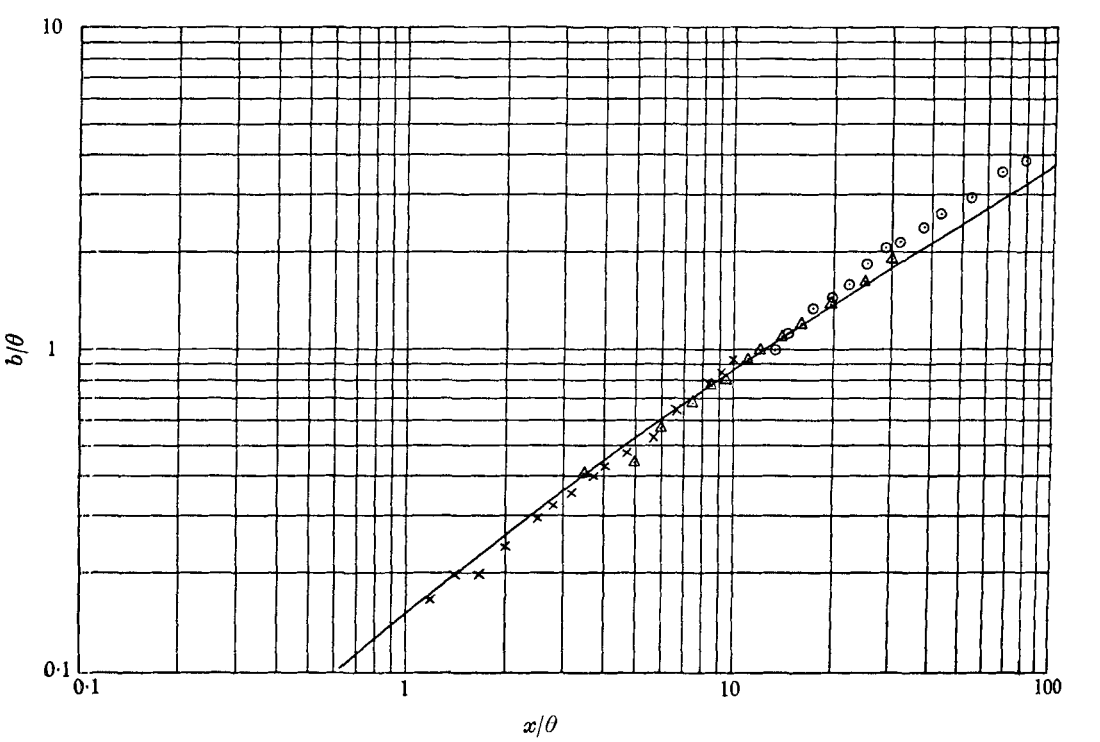

FIGURE 8. Plane jets in moving streams.
λ_0 (Weinstein): ×, 0·5; △, 1; ⊙, 2; —, theoretical, $\theta/d = (\lambda_0+1)/\lambda_0^2$.

jet in a stream of constant velocity. It may be seen that the downstream flow is predicted very well indeed for low velocity ratios λ, though at higher values of λ a distinct deviation becomes apparent. For the plane jet $U_j \propto x^{-\frac{1}{2}}$ at all λ. However, for very large λ (e.g. plane wake) the proportionality constants are quite different than for low λ. Figure 7 shows for comparison the decay of the plane wake calculated from the measured data of Schlichting.

Discussion

For both plane and axisymmetric jets immersed in constant-velocity streams it appears from experimental data that the mean velocity field can be calculated from free-jet data (by assuming the flow to be approximately self-preserving) as long as the local velocity ratio λ is less than a value of one or two. This result has bearing on the calculations described subsequently which show that for the effect of confining walls to be significant λ must be well below unity until the jet spreads to the walls. After this point, of course, self-preservation of the velocity distribution can no longer be even approximately valid.

The method described in the foregoing assumes only that the velocity and shear distribution are approximately self-preserving over the major part of the flow field. While this assumption is shown by detailed measurements of the free jet to be only approximate, it none the less provides a means of predicting the mean velocity field to quite good accuracy, under the restriction already discussed. The use of this assumption makes the method independent of the usual phenomenological theories of shear flow.

The location of the virtual origin of the jet in any actual flow will depend on the velocity distribution across the nozzle or slot exit plane. Figures 5–8 apply to jets of nearly uniform nozzle exit plane velocity and Reynolds numbers (based on nozzle diameter) exceeding at least 10^4 (Ricou & Spalding 1961). Under these conditions it appears that the virtual origin can be considered to be located in the nozzle exit plane. If, at the other extreme, the jet velocity distribution was as shown in figure 3 at the exit plane, the virtual origin would have to be shifted about eight diameters upstream.

The theoretical curves on figures 5–8 have all been calculated with the use of shear integrals derived from free-jet data, viz. $\psi_1 = 0{\cdot}0255$ (axisymmetric), $\psi_0 = 0{\cdot}0144$ (two-dimensional). When more accurate data become available it may be possible to deduce the effective variation of this shear integral with λ (supposing the velocity integrals to be still constant).

4. Axisymmetric jets in constant diameter ducts

The subject of this part of the paper is the behaviour of incompressible jet flow in ducts of constant cross-sectional area. Equations are developed for predicting axisymmetric flow only. Theoretical results are compared with the measurements of Hembold *et al.* (1954) and Becker *et al.* (1962).

If the flow field is sufficiently large the potential core region can again be replaced conceptually by a virtual source located approximately in the nozzle exit plane. Downstream of this source three distinct regions of flow must be identified, as has been done in the Introduction.

4.1. *Potential outer flow*

As a jet spreads in a constant area duct it reduces the cross-sectional area of the free stream and continuously entrains free-stream fluid. Since the relative loss of fluid from the free stream is typically greater than the relative loss of flow area, the free stream decelerates and the term in equation (4) containing the velocity gradient dU_0/dx is no longer negligible.

Integrating equation (4) for the axisymmetric jet it becomes

$$\frac{1}{U_j}\frac{dU_j}{dx}[\lambda\phi_{11}+\phi_{21}+\phi_{31}]+\frac{1}{\delta}\frac{d\delta}{dx}[3\lambda\phi_{11}+2\phi_{31}]+\frac{1}{U_0}\frac{dU_0}{dx}[\tfrac{5}{2}\lambda\phi_{11}]=\frac{\psi_1}{\delta},$$

or, since $\lambda = U_0/U_j$,

$$\frac{1}{U_j}\frac{dU_j}{dx}[\tfrac{7}{2}\lambda\phi_{11}+\phi_{21}+\phi_{31}]+\frac{1}{\delta}\frac{d\delta}{dx}[3\lambda\phi_{11}+2\phi_{31}]+\frac{1}{\lambda}\frac{d\lambda}{dx}[\tfrac{5}{2}\lambda\phi_{11}]=\frac{\psi_1}{\delta}, \qquad (11)$$

in which the constants ϕ and λ are defined as under equation (6).

If wall friction is negligible (an assumption to be justified subsequently) and the pressure $P = p+\rho\overline{u^2}$ is approximately uniform across any one transverse plane then the axial pressure gradient will be related to momentum changes by

$$0 = \pi R^2\frac{dP}{dx}+\frac{d}{dx}\int_0^R 2\pi\rho U^2 y\,dy,$$

in which R is the radius of the duct. If a radially uniform external stream exists (i.e. the jet has not yet spread to the wall) the velocity within the jet may be written

$$U = U_0+U_j f(\eta) \quad (0<\eta<1),$$

where as before $\eta = y/\delta$ and the pressure gradient is given by

$$-\frac{1}{\rho}\frac{dP}{dx} = U_0\frac{dU_0}{dx}.$$

Substituting these expressions in the momentum equation it becomes

$$0 = \pi R^2\rho\left[-d(\tfrac{1}{2}U_0^2)/dx+R^{-2}\,d(U_0^2R^2)/dx+2R^{-2}\frac{d}{dx}\left\{\delta^2U_j^2(2\lambda\phi_{41}+\phi_{51})\right\}\right].$$

If the duct radius R is constant this expression may be integrated with the result

$$\tfrac{1}{2}M = \rho U_j^2[\tfrac{1}{2}\lambda^2+2(\delta/R)^2(2\lambda\phi_{41}+\phi_{51})], \qquad (12)$$

in which $\frac{1}{2}M$ is the average sum of momentum and pressure forces per unit area, constant since the cross-sectional area of the duct is considered uniform and wall shear stresses are neglected. Equation (12) is only valid for $\lambda \geqslant 0$. For $\lambda < 0$ a different expression is required for the sum of the pressure and momentum forces since the pressure is no longer simply related to the velocity outside the jet.

The total mass flow per unit area through the duct may be written

$$m = \rho U_j[\lambda+2\phi_{41}(\delta/R)^2]. \qquad (13)$$

The two constants m and M may be combined to form an important parameter which (for $\lambda > 0$) is

$$\frac{m}{(M\rho)^{\frac{1}{2}}} = \frac{\lambda + 2\phi_{41}(\delta/R)^2}{\{\lambda^2 + 4(2\phi_{41} + \phi_{51})(\delta/R)^2\}^{\frac{1}{2}}}. \tag{14}$$

It will now be shown that the behaviour of jets confined in constant-area ducts can be expressed as a function of only two independent variables, i.e. $m/(M\rho)^{\frac{1}{2}}$ and x/D, in which D is the duct diameter. From equation (13) it may be seen that

$$\frac{1}{U_j}\frac{dU_j}{dx} = \frac{d\lambda/dx + 4\phi_{41}\,\delta(d\delta/dx)/R^2}{\lambda + 2(\delta/R)^2\phi_{41}}$$

Then, by reason of this relationship, equation (11) can be expressed in the form

$$q_1(\lambda, \delta/R)\,d\lambda/dx + q_2(\lambda, \delta/R)\,d\delta/dx = \psi_1/\delta,$$

in which the coefficients q_1 and q_2 depend only on the variables λ and (δ/R). Now equation (14) may, in principle, be employed to eliminate (δ/R) from the above relationship with the result

$$q_3[\lambda, m/(M\rho)^{\frac{1}{2}}]\,d\lambda/dx = \psi_1/\delta.$$

Thus, the assumption of self-preservation leads to the dependence of both λ and δ/D on x/D and $m/(M\rho)^{\frac{1}{2}}$ only. From equation (12) it then becomes clear that the dimensionless velocities $U_j/(M/\rho)^{\frac{1}{2}}$ and $U_0/(M/\rho)^{\frac{1}{2}}$ can also be expressed as functions of these two independent variables.

Evaluated in the exit plane of the nozzle for uniform jet and secondary streams

$$\frac{m}{(M\rho)^{\frac{1}{2}}} = \frac{\lambda_0 + (d/D)^2}{\{\lambda_0^2 + 2(1 + 2\lambda_0)(d/D)^2\}^{\frac{1}{2}}},$$

in which d is the nozzle diameter, D the duct diameter and λ_0 the initial velocity ratio. The numerical value of $m/(M\rho)^{\frac{1}{2}}$ should normally lie between zero and one. A value of zero signifies no net mass flow in the pipe, i.e. a jet issuing into a pipe whose downstream end is closed. Values of $m/(M\rho)^{\frac{1}{2}}$ approaching unity signify that the ratio d/D is negligible so that influence of the walls is insignificant. The dimensionless group $m/(M\rho)^{\frac{1}{2}}$ as defined by equation (14) is uniquely related to equivalent variables proposed by Curtet & Craya (1955), and Spalding.

In order to calculate the development of the jet flow, equation (11), the momentum integral equations, and the continuity equation may together be expressed as

$$\begin{bmatrix} \alpha_0 & \alpha_1 & \alpha_2 \\ \alpha_3 & \alpha_4 & \alpha_5 \\ \alpha_6 & \alpha_7 & \alpha_8 \end{bmatrix} \begin{bmatrix} U_j'/U_j \\ \lambda'/\lambda \\ \delta'/\delta \end{bmatrix} = \begin{bmatrix} \psi_1/(\delta/D) \\ 0 \\ 0 \end{bmatrix}, \tag{15}$$

in which the primes signify differentiation with respect to x/D and the coefficients α_n are given by

$$\begin{aligned} &\alpha_0 = \tfrac{7}{2}\lambda\phi_{11} + \phi_{21} + \phi_{31}, \quad &&\alpha_1 = \tfrac{5}{2}\phi_{11}, \quad &&\alpha_2 = 3\lambda\phi_{11} + 2\phi_{31}, \\ &\alpha_3 = 3\lambda + 2\phi_{51}/\phi_{41}, &&\alpha_4 = 2\lambda, &&\alpha_5 = 2\lambda + 2\phi_{51}/\phi_{41}, \\ &\alpha_6 = \lambda + 8\phi_{41}(\delta/D)^2, &&\alpha_7 = \lambda, &&\alpha_8 = 16\phi_{41}(\delta/D)^2. \end{aligned}$$

The values of the integrals $\psi_1, \phi_{11}, \ldots, \phi_{51}$ have been derived in § 3 of this paper from free-jet data, from which it is also concluded that a reasonable value of δ/b is 1·44. Using these numerical values, calculations based on (15) and using the Runge–Kutta–Merson procedure have been performed on a digital computer and are presented in figures 9–13. Discussion of these results and comparison with experimental data will follow a description of methods of dealing with the other two regions of the jet flow field.

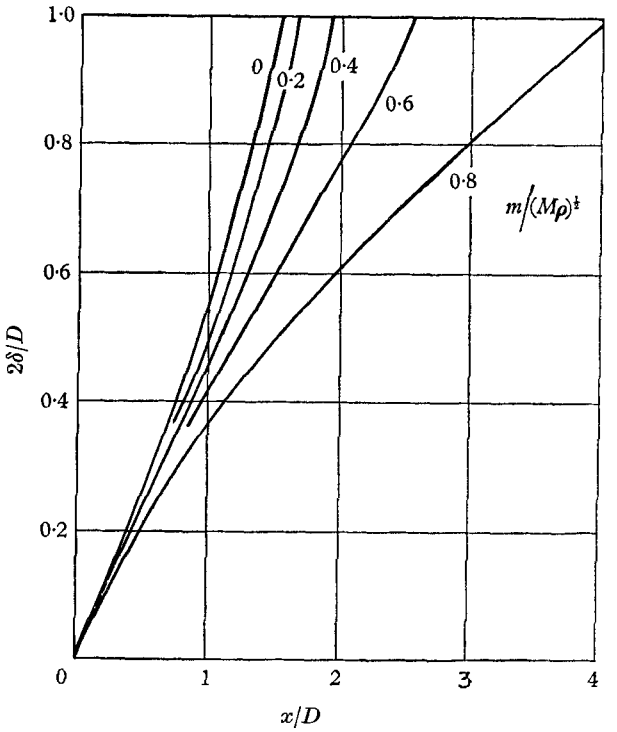

FIGURE 9. Axisymmetric jet in a constant-diameter tube.

4.2. *Recirculation region*

In this region of partially reversed flow (zone C in figure 1) it is no longer possible to consider the pressure gradient and the free-stream velocity to obey

$$-\rho^{-1}dP/dx = U_0 dU_0/dx.$$

However, experiments show that in this recirculation region it is approximately true that the static pressure is constant through the region. Furthermore, the jet shape is approximately retained so that with appropriate modification the foregoing equations may also be used to predict the jet behaviour in the recirculation region. Considering the flow external to the jet uniform even when it is reversing is of course a considerable approximation.

4.3. *Wall-jet interaction*

When the jet has spread to the wall it begins to undergo considerable changes in its velocity and shear distributions so that the preceding equations are no longer

useful. Further the 'free-stream' has disappeared so the static pressure in the duct can no longer be linked to the velocity U_0 even in the absence of recirculation.

According to Townsend, the assumption that the eddy viscosity defined by

$$\nu_T = -\overline{u'v'}/(\partial U/\partial y)$$

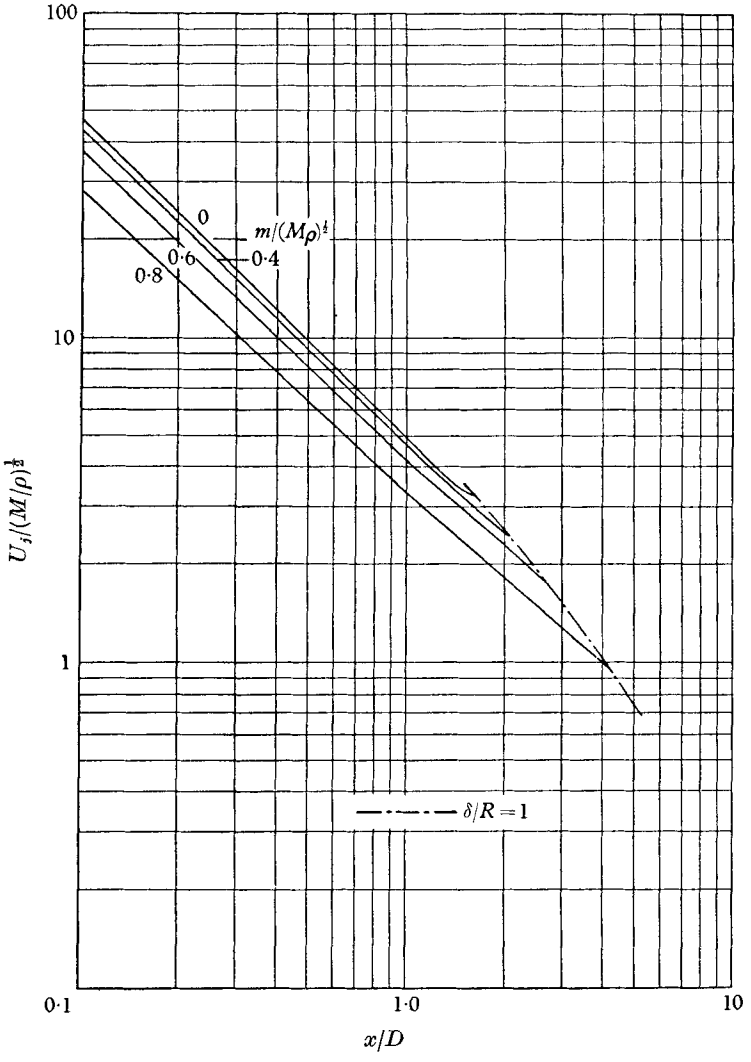

FIGURE 10. Axisymmetric jet flow in a constant-area duct.

is uniform across the width of the shear layer leads to remarkably accurate predictions of the mean velocity field of self-preserving free turbulent shear flows. For the free axisymmetric jet, Hinze (1959) has calculated the radial distribution of eddy viscosity and it appears that the mean value decreases somewhat near the edge of the jet. However, if the local eddy viscosity were divided by the local intermittency factor the result would be fairly uniform indeed across the shear layer. Townsend suggests there are no physical reasons for justifying this result, but it is notable because it leads to useful simplifications.

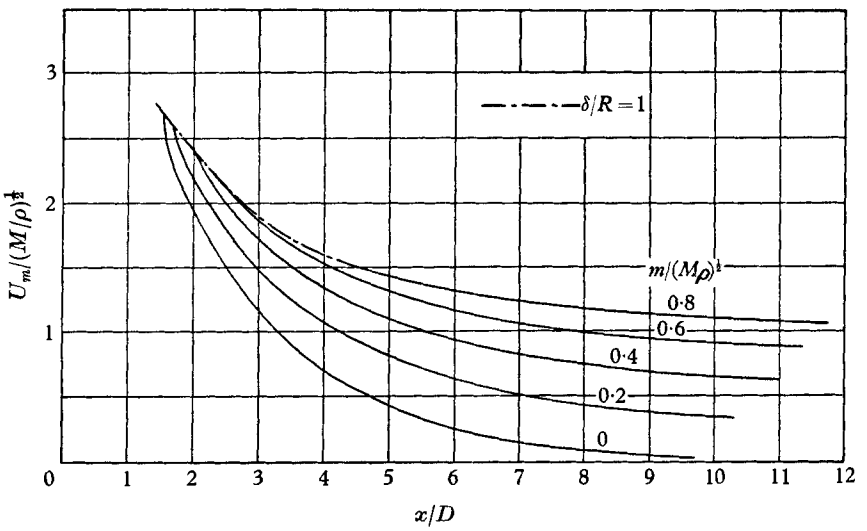

FIGURE 11. Axisymmetric jet flow in a constant-area duct; centre-line velocity.

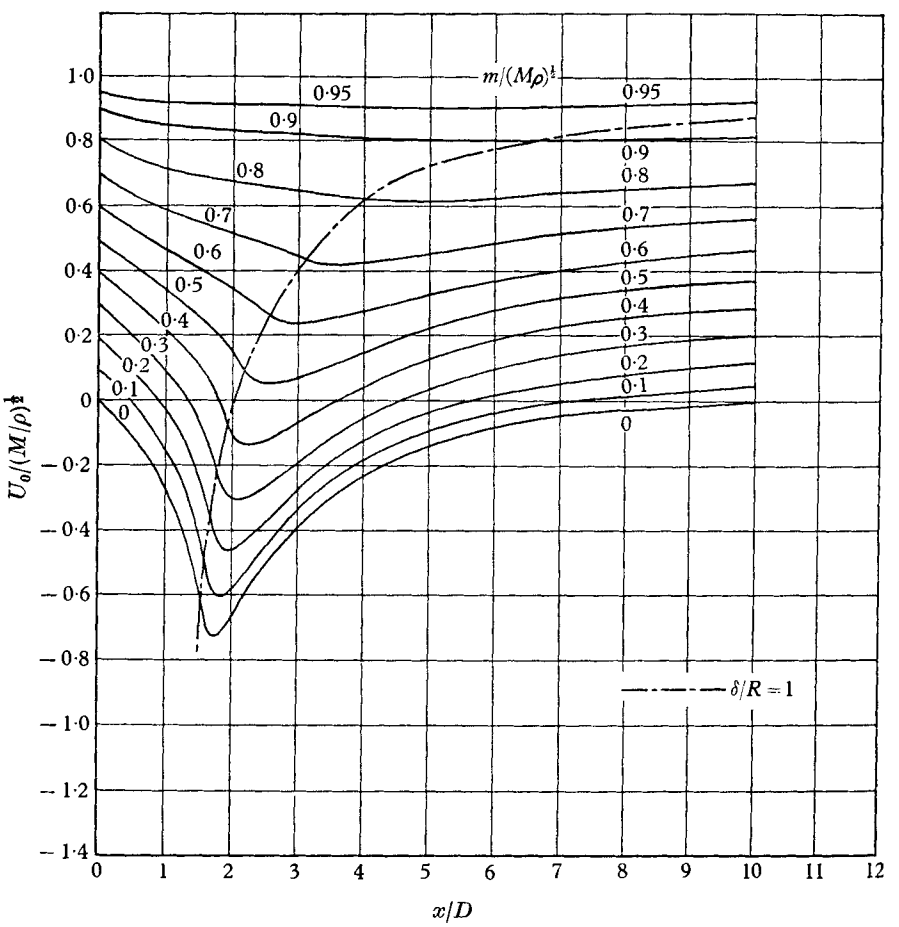

FIGURE 12. Axisymmetric jet flow in a constant-diameter tube; velocity near wall.

In the following calculation it will be assumed that the effective eddy viscosity distribution in this region of developing flow is given by

$$\nu_T = \text{const.}\, U_j R g_1(\eta), \tag{16}$$

in which the function g_1 roughly approximates the result of Hinze's calculation, i.e.

$$g_1 = 1 \quad (0 < \eta < 0{\cdot}28),$$

and

$$g_1 = 1{\cdot}191 - 0{\cdot}684\eta, \quad 0{\cdot}28 < \eta < 1,$$

where

$$\eta = y/R.$$

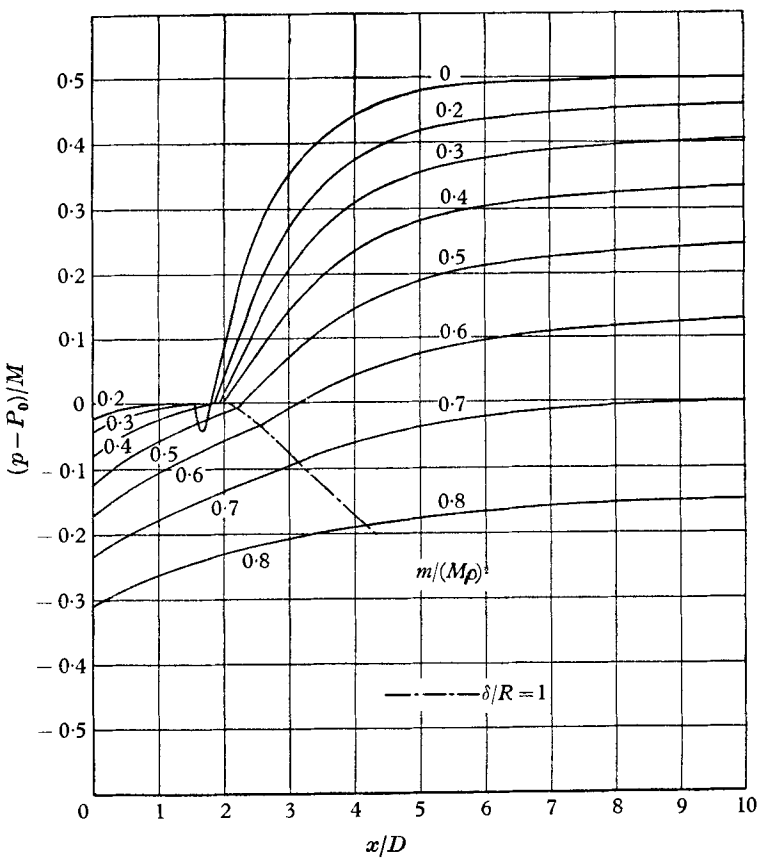

FIGURE 13. Axisymmetric jet flow in a constant-diameter tube; pressure.

The constant in equation (16) is evaluated from free-jet data. The support that is offered for the assumption is simply that it provides a reasonably good prediction of the mean velocity field, as will be shown.

In order to allow for the first-order effects of a change in velocity distribution in this zone of the flow the velocity may be set equal to

$$U = U_0 + U_j[f(\eta) + \xi g(\eta)], \quad \eta = y/R, \tag{17}$$

in which U_0 is the velocity near the wall (the wall boundary layer is ignored), U_j is the difference between U_0 and the maximum velocity and ξ is a function of x only.

If the function $f(\eta)$ is arbitrarily selected as the one which was used for the preceding zones, then ξ equals zero when the jet 'touches' the wall and is a measure of the change in shape of the velocity profile thereafter. If the function $g(\eta)$ is only required to satisfy the boundary conditions

$$g(0) = g'(0) = 0; \quad g(1) = g'(1) = 0,$$

then a simple function may be used, e.g.

$$g(\eta) = \eta^2(1-\eta)^2.$$

Within limits the choice of the function $g(\eta)$ will not be of great importance.

In the preceding calculations three variables U_j, λ, and δ were determined by the use of continuity and momentum integral equations and by means of the moment-of-momentum integral equation. For the present case four unknowns may be identified: U_j, λ, ξ and P. To form the necessary four equations it is possible this time to take in addition to the continuity equation three successive integrals of the momentum equation. This may be done by multiplying equation (1) by y^j where $j = 1, 2, 3$ and integrating with respect to y. Using equations (16) and (17) the results may be expressed in the form

$$\begin{bmatrix} \beta_0 & \beta_1 & \beta_2 & \beta_3 \\ \beta_4 & \beta_5 & \beta_6 & \beta_7 \\ \beta_8 & \beta_9 & \beta_{10} & \beta_{11} \\ \beta_{12} & \beta_{13} & \beta_{14} & \beta_{15} \end{bmatrix} \begin{bmatrix} \overline{U'}/U_j \\ \lambda' \\ \xi' \\ \overline{P'} \end{bmatrix} = \begin{bmatrix} \beta_{16} \\ \beta_{17} \\ \beta_{18} \\ \beta_{19} \end{bmatrix}, \tag{18}$$

in which the prime signifies differentiation with respect to x/D and $\overline{P}$ is the dimensionless variable $2P_0/M$ and $\overline{U}_j$ is the variable $U_j/(M/\rho)^{\frac{1}{2}}$. In general the coefficient matrix elements β have the form

$$\beta_n = a_{1n}\lambda^{-2} + a_{2n}\lambda + a_{3n}\lambda^2 + a_{4n}\lambda\xi + a_{5n}\xi^2 + a_{6n},$$

in which the coefficients $a_{1n}, \ldots, a_{6n}$ depend only on various integrals across the shear layer of the velocity and shear distribution functions $f(\eta)$, $g(\eta)$, and $g_1(\eta)$. From (18) the derivatives $\overline{U}_j$, λ', ξ', and $\overline{p}'$ were evaluated. Calculations were performed on a digital computer again using the Runge–Kutta–Merson integration procedure.

4.4. *Results of calculations*

Figure 9 shows the spreading of axisymmetric jets in tubes. As may be seen from figure 3 the 'edge' of the jet can only be defined arbitrarily. Nevertheless, it is necessary to make such a definition to decide when the jet has attached to the wall. It may be seen that for $m/(M\rho)^{\frac{1}{2}}$ above 0·6 the jet spreading becomes decidedly non-linear which is not in accord with the proportionality (5). Thus the assumption of approximate self-preservation of the flow prior to jet attachment can only be valid below a limiting value of $m/(M\rho)^{\frac{1}{2}}$. Figure 10 shows the axial variation of jet velocity U_j in the same zone. For moderate values of $m/(M\rho)^{\frac{1}{2}}$ it too satisfies (5). Figure 11 shows the decay of centre-line velocity in the region after the jet has attached to the wall. It may be noted that the decay rate is typically very much higher for low values of $m/(M\rho)^{\frac{1}{2}}$.

The free-stream velocity U_0 is given by figure 12. For $m/(M\rho)^{\frac{1}{2}} < 0{\cdot}45$ it is possible to have a region of recirculation. Figure 12 can only be approximate in the region of recirculation due to the simplifications employed in the calculations. Nevertheless, it will be shown to be supported to some extent by experimental data. After the jet touches the wall, pressure gradients are rapidly established even though the flow near the wall may still be recirculating. This is shown by figure 13. For $m/(M\rho)^{\frac{1}{2}} < 0{\cdot}4$ most of the overall pressure rise has

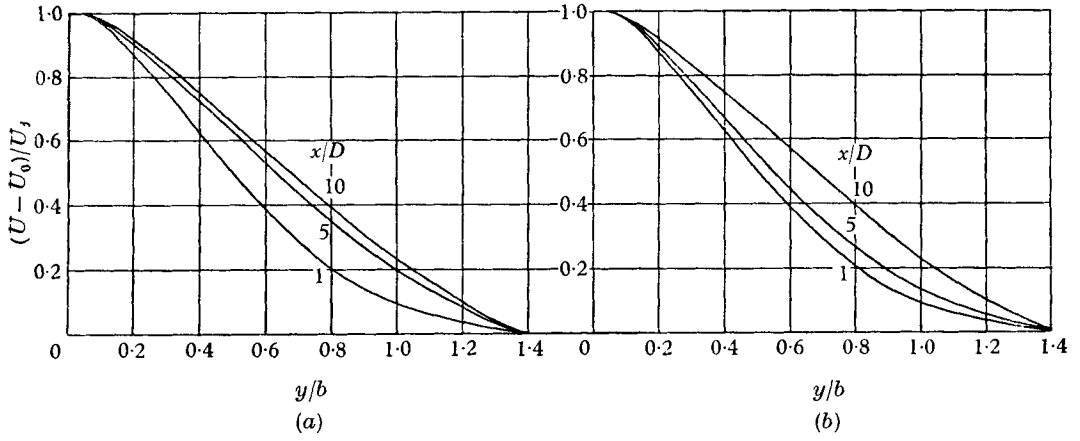

FIGURE 14. Axisymmetric jet flow in a constant-diameter tube; typical velocity distribution. (*a*) $m(M\rho)^{\frac{1}{2}} = 0{\cdot}2$; (*b*) $m/(M\rho)^{\frac{1}{2}} = 0{\cdot}8$.

taken place before the wall flow has been returned to the forward direction. It may be shown that the pressure of the stream after mixing is completed is given by

$$(p-P_0)/M = \tfrac{1}{2} - m^2/M\rho.$$

Figure 14 shows typical velocity profiles; the distribution does not alter radically even after the jet has touched the wall, confirming that within certain limits the choice of the function $g(\eta)$ is not of great importance. From figures 10 and 12 it may be seen that in the region before the jet attaches λ is always less than unity for $m/(M\rho)^{\frac{1}{2}} < 0{\cdot}8$. Thus according to the conclusion of § 3 it might be expected that these results would be reasonable in such a range.

4.5. *Comparison with experimental data*

The foregoing results are compared in figures 15 and 16 with experimental data most of which has been obtained by Hembold *et al.* (1954). They measured the wall pressure distribution along a 6-inch diameter tube with air jet and secondary streams and maximum velocities of the order of a few hundred ft./sec. The ratio of their nozzle and tube diameters was 0·10. The data points for $m/(M\rho)^{\frac{1}{2}} = 0$ were obtained by the author using a closed-end pipe about 2 in. in diameter and 24 in. long, with air injected through a concentric nozzle. The ratio of nozzle-to-tube diameter was 0·125 for that test.

In general the calculated and measured distributions are in quite good agreement so that equation (16) seems to be a satisfactory approximation. The greatest

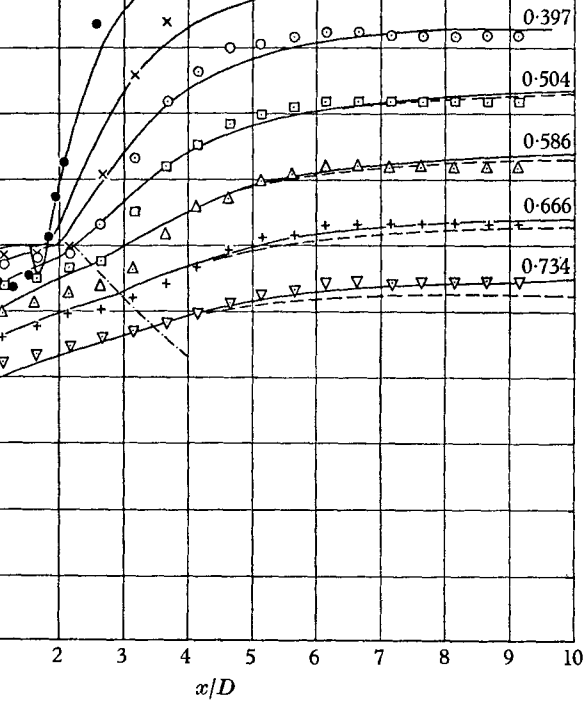

xperimental and theoretical wall pressure distributions. Hembold): ×, 0·275; ⊙, 0·397; ⊡, 0·504; △, 0·586; +, ; —, theoretical; – – – –, theoretical ($C_f = 0{\cdot}004$); —·—,

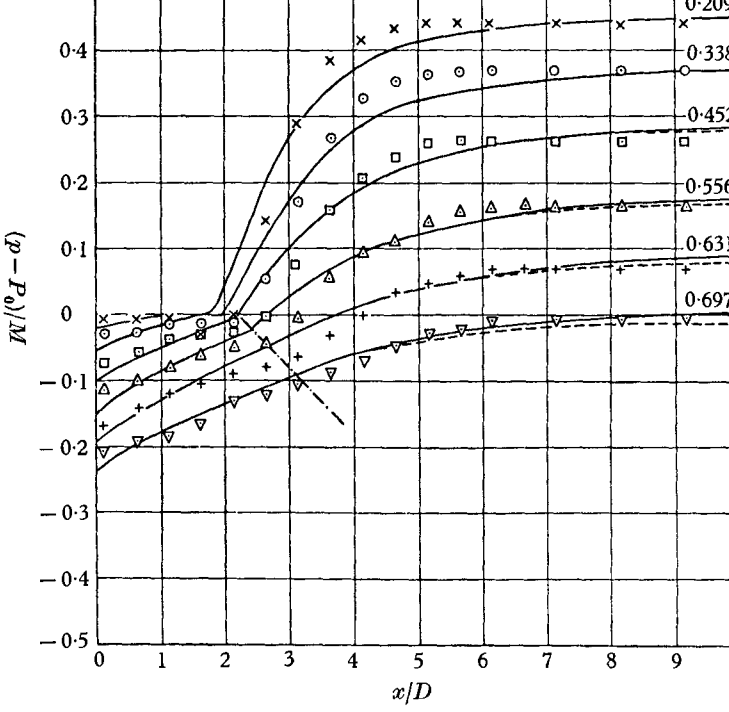

FIGURE 16. Experimental and theoretical wall pressure distributions. (Hembold): ×, 0·209; ⊙, 0·338; ⊡, 0·452; △, 0·556; +, 0·631; ▽, 0 theoretical; – – –, theoretical ($C_f = 0{\cdot}004$); —·—, $\delta/R = 1$.

discrepancies are for low values of $m/(M\rho)^{\frac{1}{2}}$ suggesting that the assumptions which have been made herein regarding the recirculation zone are inadequate. Some improvement in the solution might be made by arbitrarily altering the definition of the jet 'edge' (figure 3) but what seems most needed is a more detailed experimental study of the regions of recirculation and attachment.

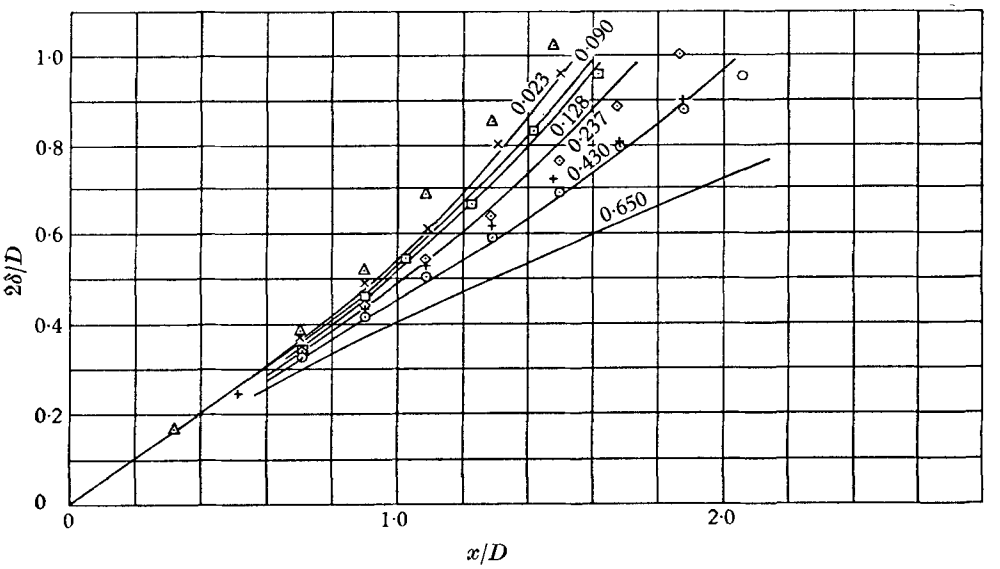

FIGURE 17. Experimental and theoretical variations in jet width. $m/(M\rho)^{\frac{1}{2}}$ (Becker): △, 0·023; ×, 0·090; □, 0·128; ◇, 0·237; +, 0·430; ⊙, 0·653; —, theoretical.

The wall shear stress only exerts an appreciable effect on the flow at high values of $m/(M\rho)^{\frac{1}{2}}$ as is shown in figures 15 and 16 from the results of calculations using a constant value of the shear stress coefficient C_f defined by

$$C_f = \tau_w/\tfrac{1}{2}\rho U_0^2,$$

in which τ_w is the wall shear stress. The reason the wall shear stress affects the pressure rise so little is that the latter is only significant when λ_0 is so small that the wall stress τ_w is small compared to other terms in the axial momentum integral equation. No account was taken of wall boundary-layer displacement thickness which would tend to reduce the pressure recovery. The effect appears small.

Figure 17 shows Becker's measurements of jet width, which are in general agreement with the present calculations except for one value of $m/(M\rho)^{\frac{1}{2}}$. Figure 18 indicates Becker's measurements of the free-stream velocity U_0. Measurements in the recirculation region may be difficult due to unsteadiness of the flow, but the measurements are in reasonable agreement with the calculations except at high values of $m/(M\rho)^{\frac{1}{2}}$. Figure 19 shows the data of Landis & Shapiro replotted in co-ordinates which take into account the influence of the duct walls.

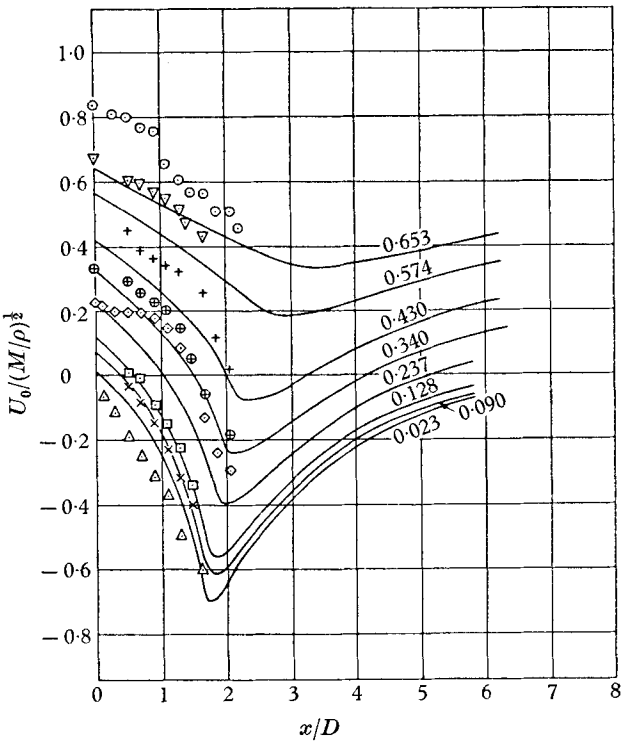

FIGURE 18. Experimental and theoretical variations in velocity near the wall. $m/(M\rho)^{\frac{1}{2}}$ (Becker): △, 0·023; ×, 0·090; □, 0·128; ◇, 0·237; ⊕, 0·340; +, 0·403; ▽, 0·574; ⊙, 0·653; —, theoretical.

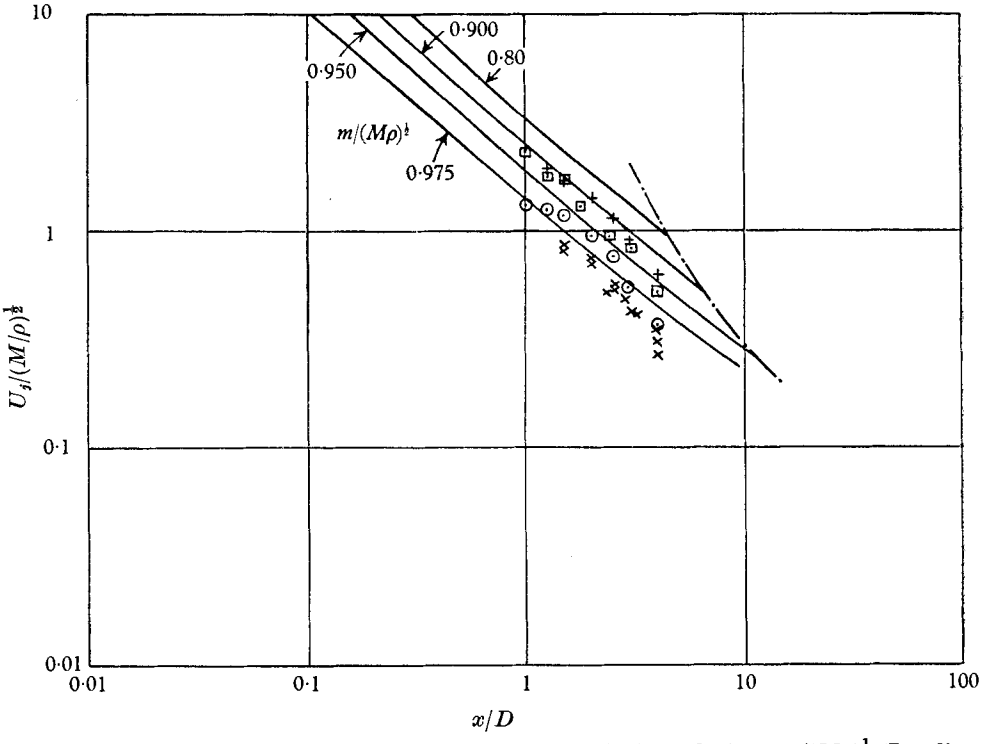

FIGURE 19. Experimental and theoretical variations in jet velocity. $m/(M\rho)^{\frac{1}{2}}$ (Landis–Shapiro): ×, 0·977; ⊙, 0·965; □, 0·888; +, 0·87; —, theoretical; —·—, $\delta/R = 1$.

5. Conclusions

1. The use of self-preservation hypothesis permits the mean velocity field of jets surrounded by constant-velocity streams to be calculated from free-jet data, as long as the ratio of the external velocity to the maximum jet relative velocity does not exceed one or two. In this way the jet velocity ratio U/U_j and the thickness ratio δ/θ can be shown to depend only on x/θ.

2. In the absence of recirculation a reasonable prediction of the behaviour of turbulent confined jets can be made with the following assumptions:

(*a*) approximate self-preservation of the flow up to the point at which the jet attaches to the wall;

(*b*) negligible influence of wall boundary layers;

(*c*) potential outer flow until the jet attaches (except in the recirculation region);

(*d*) constant pressure in the recirculation region;

(*e*) use of a similar eddy viscosity distribution and a two-parameter velocity distribution after the jet touches the wall;

(*f*) evaluation of all shear integrals from free-jet data.

3. Experimental studies of velocity and shear distributions in the zones of jet recirculation and in the vicinity of jet attachment to the wall are desirable in order that prediction of these confined jet flows can be improved.

The author acknowledges with gratitude the financial support of the John Simon Guggenheim Memorial Foundation during the period in which this study was made. He is also grateful to Mr Dennis McConalogue for considerable advice on computation procedures and would like to acknowledge several helpful discussions with Prof. D. B. Spalding on the general subject of ducted jets.

Appendix. Two-dimensional (plane) jet in a constant-velocity stream

In the same way as for the axisymmetric jet, equation (7) may be used to eliminate δ from equation (6) for the two-dimensional case ($i = 0$). The resulting expression may be integrated and expressed in the form

$$\frac{x}{\theta} = \frac{\phi_{10}}{2\psi_0\phi_{40}}\left[\frac{\Lambda^2}{2} - \frac{\phi_{20}}{\phi_{10}}\Lambda + \frac{\phi_{50}}{\phi_{40}}\left\{\left(\frac{\phi_{20}+\phi_{30}}{\phi_{10}}\right) - 3\frac{\phi_{50}}{\phi_{40}}\right\}\ln\Lambda + \left(\frac{\phi_{50}}{\phi_{40}}\right)^2\left(2\frac{\phi_{50}}{\phi_{40}} - \frac{\phi_{30}}{\phi_{10}}\right)\Lambda^{-1}\right] + C_0, \qquad \text{(A 1)}$$

in which $$\Lambda = \lambda + \phi_{50}/\phi_{40},$$

and C_0 is the constant of integration. To evaluate the functions $\phi_{10}, \ldots, \phi_{50}$ it would be best to use accurate data on the velocity profile of the two-dimensional free jet. However, if for convenience a cosine curve is used to approximate the velocity distribution, the appropriate integrals are

$$\phi_{10} = \tfrac{1}{4} - 1/\pi^2, \quad \phi_{20} = \tfrac{3}{16} - 1/\pi^2, \quad \phi_{30} = \tfrac{5}{16} - 1/\pi^2, \quad \phi_{40} = \tfrac{1}{2}, \quad \phi_{50} = \tfrac{3}{8}.$$

The shear integral ψ_0 may, as before, be deduced from equations (3) and (6):

$$2\psi_0 = (\phi_{30} - \phi_{20})\,(d\delta/dx)_{\lambda=0}.$$

From Reichhardt's data the spreading of the free jet is given by

$$db/dx = 0{\cdot}23.$$

For the cosine velocity distribution $d\delta/dx = db/dx$. Thus using the given values of ϕ_{20}, ϕ_{30} and $(db/dx)_{\lambda=0}$

$$\psi_0 = 0{\cdot}0144.$$

The constant of integration is again determined by the condition that at the virtual origin $x = 0$ and $\lambda = 0$.

With these numerical values the two-dimensional jet behaviour may be determined from

$$x/\theta = 5{\cdot}14\Lambda^2 - 5{\cdot}97\Lambda - 3{\cdot}34\ln\Lambda - 0{\cdot}460\Lambda^{-1} + 1{\cdot}64, \qquad \text{(A 2)}$$

in which

$$\Lambda = \lambda + 0{\cdot}75$$

and θ may be determined from conditions at the nozzle exit plane

$$\theta/d = (\lambda_0 + 1)/\lambda_0^2,$$

in which d is the width of slot from which the jet issues and λ_0 is the initial velocity ratio.

REFERENCES

Becker, H. A., Hottel, H. C. & Williams, G. C. 1962 *Proc. Ninth Int. Symp. Combustion*, Cornell.

Craya, A. & Curtet, R. 1955 *C.R. Acad. Sci., Paris*, **241**, 621.

Curtet, R. 1958 *Combustion and Flame*, **2**, 383–411.

Ferguson, C. K. 1949 *Proc. Heat Transf. & Fluid Mech. Inst.*, Berkeley.

Forstall, W. J. & Shapiro, A. H. 1950 *J. Appl. Mech.* **17** (*Trans. ASME*, **72**), 399.

Hembold, H. B., Luessen, G. & Heinrich, A. M. 1954 An experimental comparison of constant pressure and constant diameter jet pumps. *Engng Rep.* no. 147, *Univ. of Wichita, School of Engineering.*

Hinze, J. O. 1959 *Turbulence—An Introduction to its Mechanism and Theory.* New York: McGraw Hill.

Kryzwoblocki, M. Z. 1956 *Jet Prop.* **26**, 970.

Landis, F. & Shapiro, A. H. 1951 *Proc. Heat Transf. & Fluid Mech. Inst.*, no. 133.

Pabst, O. 1944 *Die Ausbreitung heissen Gasstrahlen in bewegten Luft*, II, Teil Um 8007.

Ricou, F. P. & Spalding, D. B. 1961 Measurements of entrainment by axisymmetrical turbulent jets. *J. Fluid Mech.* **11**, 21–32.

Schlichting, H. 1958 *Boundary Layer Theory.* London: Pergamon Press.

Spalding, D. B. 1958 *Seventh Int. Symp. on Combustion.* Oxford: Butterworth Scientific Publications.

Squire, H. B. & Trouncer, J. 1944 Round jets in a general stream. *Aero. Res. Counc. Tech. Rep. R & M*, no. 1974.

Szablewski, W. 1946 *NACA TM* 1288. (Translation of 'Die Ausbreitung eines Heissluftstrahles in bewegten Luft', GDC/2460.)

Tetervin, N. & Lin, C. C. 1951 *NACA Rep.* no. 1046.

Townsend, A. A. 1956 *The Structure of Turbulent Shear Flow.* Cambridge University Press.

Weinstein, A. S., Osterle, J. F. & Forstall, W. 1956 *J. Appl. Mech.*